




Article

Meteorological Factors Controlling ^7Be Activity Concentrations in the Atmospheric Surface Layer in Northern Spain

Natalia Alegría ^{1,*}, Miguel Ángel Hernández-Ceballos ², Margarita Herranz ¹,
Raquel Idoeta ¹ and Fernando Legarda ¹

¹ Department of Energy Engineering, University of the Basque Country, 48013 Bilbao, Spain; m.herranz@ehu.es (M.H.); raquel.idoeta@ehu.es (R.I.); f.legarda@ehu.es (F.L.)

² Department of Physics, University of Cordoba, 14071 Córdoba, Spain; f92hecem@uco.es

* Correspondence: natalia.alegria@ehu.es; Tel.: +34-94-601-7279

Received: 5 November 2020; Accepted: 6 December 2020; Published: 10 December 2020



Abstract: This work presents the analysis of weekly ^7Be activity concentrations in the air measured in Bilbao (northern Spain) by collecting aerosols in filters over a ten years period (2009–2018). ^7Be level is in the 0.35–7.3 mBq/m³ range, with a mean of 3.20 ± 1.12 mBq/m³. The trend, cycle, seasonal and monthly variability are evaluated using time series analysis techniques. The results indicate the impact of sunspots (24th solar cycle) on interannual ^7Be activity concentrations, and a significant seasonal and monthly variation, with maximum concentrations occurring in spring-summer and minimum in the winter. The correlation of different ^7Be ranges with local meteorological parameters, such as precipitation, temperature, relative humidity, and pressure, is also addressed, with precipitation having the greatest impact on ^7Be activity values. The analysis of synoptic airflows, by calculating the back-trajectory clusters, and local winds at surface level reveals the important influence of the arrival of slow northwest Atlantic flows and the development of breezes on reaching high ^7Be activity concentrations in this area.

Keywords: Beryllium-7; time series analysis; airflow patterns; local meteorological conditions

1. Introduction

Beryllium-7 (^7Be), a cosmogenic isotope with a half-life of 53.6 days, is one of the natural radionuclides most widely measured around the world. Once produced, ^7Be attaches to submicron-sized aerosol particles peaking in the accumulation mode [1]. Then, its measurements can be used as a proxy to study and characterize atmospheric processes, such as wet and dry deposition [2], origin of air masses [3], and to validate atmospheric transport modeling systems [4]. Two examples of monitoring and storage ^7Be data are the International Monitoring System (IMS) developed by the Comprehensive Nuclear-Test-Ban Treaty Organization (CTBTO) [5] and the Radioactivity Environmental Monitoring Database (REMDB) [6], maintained by the European Commission—Joint Research Center [7].

Due to the nature of its production, as a result of the spallation of nitrogen and oxygen nuclei by components of an atmospheric cascade induced by the galactic cosmic rays [8], ^7Be concentrations increases with height (2/3 of the total amount is produced in the stratosphere) [9]. It has a maximum production at 15 km altitude, where cosmic rays are strongly attenuated by the atmosphere. Once produced, ^7Be is rapidly attached to aerosol particles and further transported to the Earth's surface by atmospheric vertical mixing. However, the complexity of the interactions of all mechanisms modulating ^7Be concentrations near the surface makes it difficult to understand its surface temporal and spatial variability. Previous studies have already described the connection of ^7Be concentrations in the

lower troposphere and solar activity [10], wet scavenging [11], the exchange between the stratosphere and the troposphere [12], the tropospheric vertical mixing [13], and the horizontal transport [14].

Many studies have evaluated ^7Be concentrations in surface air and its relationship with meteorological factors at different scales across the Iberian Peninsula. Analysis carried out in the west (in Lisbon [15]), in the east (in Valencia [16]; in Barcelona [14]) and in the south (in Huelva [17]; in Huelva and Cordoba [18]; in Malaga [19,20]; in Granada [21]) provide a wide mosaic about the spatial distribution and the meteorological conditions regulating the temporal and seasonal variations of ^7Be in surface air in the Iberian Peninsula. In the northern part, where climatic conditions are quite different from those prevailing in more southern latitudes, the number of studies analyzing ^7Be activity concentrations, but its link with meteorological factors are scarce. To the authors' knowledge, Alegria et al., 2010 [22] is the only published article, in which the temporal behavior of ^7Be activity concentrations in the air measured was analyzed in this area (between 2001 and 2009). In Hernandez-Ceballos [23], ^7Be concentrations from 2001 to 2010 in Bilbao and in other sampling sites in Spain, were used to identify synoptic patterns associated with regional stratospheric-tropospheric transport events. The influence of meteorological factors on the variability of ^7Be activity concentrations is, hence, not well known in this area yet.

The main aim of the present study is to analyze ^7Be activity concentrations in the air measured in Bilbao (northern Spain), and to investigate the influence of synoptic and local weather factors on its temporal variability. For this purpose, and to have an adequate degree of representativeness of the results obtained, a decadal time series (2009–2018) of weekly collected aerosols in filters, meteorological surface parameters (wind direction and speed, temperature, relative humidity, and rainfall), and backward trajectories at Bilbao were evaluated. The following research issues associated with ^7Be activity concentrations in surface air are addressed:

- To characterize the temporal variability of ^7Be activity concentrations in surface air;
- To identify the airflow patterns causing different ^7Be levels;
- To investigate local meteorological factors driven ^7Be activity concentrations;

This paper is organized as follows. Section 2 describes the measurement site, the radioactivity measurements, and the meteorological data and tools used in the analysis. Section 3 presents, firstly, the results of analyzing ^7Be activity concentrations, and its correlation with local meteorological parameters, and secondly, the synoptic and local weather patterns associated with ^7Be measurements. Finally, the summary and conclusions are shown in Section 4.

2. Experiments

2.1. Study Area

Bilbao is a city located in the Basque Country region, northern Spain (Figure 1). This is a mountainous coastal area at the Gulf of Biscay (North Atlantic) and the Pyrenees mountains. The city is about 16 km away from the sea in the narrow valley of the Nervion river. The valley is flanked by low mountains rising in heights between 300 and 800 m that increases up to 1500 m away from the city. The valley channels airflows in an NW-E/ESE direction, prevailing NW winds in the summertime and veering to E/ESE in autumn and winter. On a daily basis, and mainly on spring and summer days, thermal sea-land breezes develop along the valley.

Temperatures are quite mild in this area, with an average value of 8 °C in winter and 20 °C in the summertime [24]. Precipitation is inhomogeneously distributed over the year, with January, February, and November registering averages between 150 and 200 L/m², while in July and August, the averages remain in 30 L/m². The mean annual rainfall for the studied period amounts to 1085 L/m².

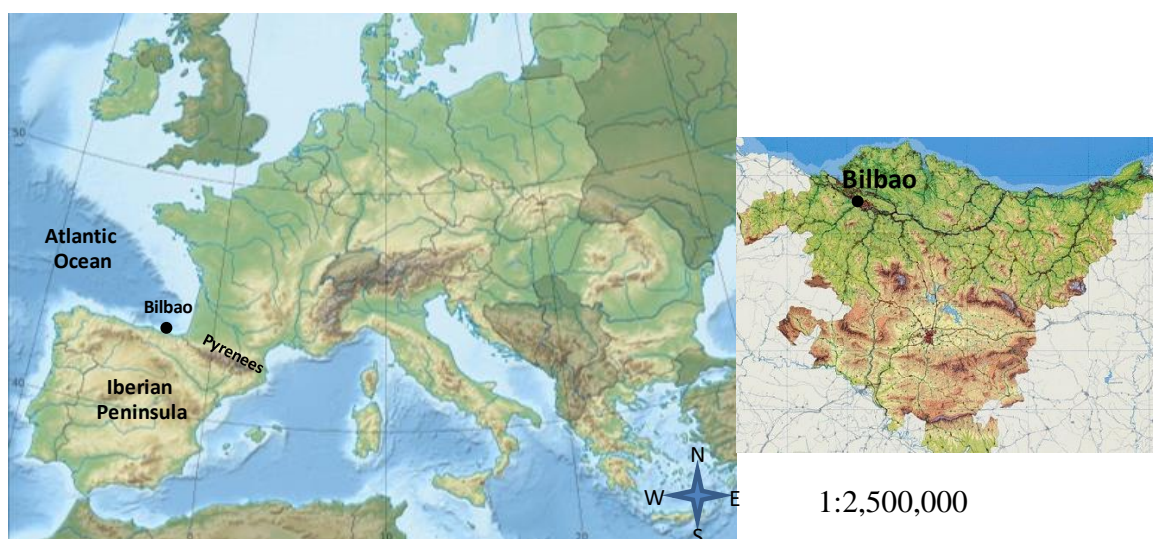


Figure 1. Location of the sampling site in the northern area of the Iberian Peninsula. (Figure 1 is licensed under the Creative Commons Attribution-Share Alike 3.0 Unported license, https://commons.wikimedia.org/wiki/File:European_Union_relief_laea_location_map.svg).

2.2. ^7Be Activity Concentration Measurements and Meteorological Data

The activity of ^7Be and meteorological parameters have been measured in a monitoring station sited in Bilbao city (43.26 N, -2.94 W). Figure 2 shows the aerosol sampler and the meteorological station, located on the roof of the Faculty of Engineering (34 m above sea level).



Figure 2. Photography of the sampling place on the roof of the Faculty of Engineering.

Atmospheric airborne aerosols are collected using a high volume sampler whose nominal flow rate is $500 \text{ m}^3/\text{h}$. This sampler uses a polypropylene filter ($44 \times 44 \text{ cm}$ in size and $0.8 \text{ }\mu\text{m}$ pore size), which is replaced weekly. After removing the filter from the sampler, a gamma spectrometric measurement is carried out using an HPGe detector (90% efficiency) with a resolution better than 2.2 keV FWHM for the 1332 keV gamma line of ^{60}Co . A calibration source was prepared “ad hoc” with the same type of filter as used. The counting time has been $2.5 \times 10^5 \text{ s}$, and that time allows us to get detection limits between 1.53×10^{-6} and $2.05 \times 10^{-5} \text{ Bq/m}^3$ and uncertainties, with a coverage factor $k = 2$, between 5.82×10^{-6} and $6.98 \times 10^{-4} \text{ Bq/m}^3$. In the present study, 496 samples collected from January 2009 to December

2018 were used. These data are also stored in the Radioactivity Environmental Monitoring Database (REMdb) supported by the European Commission—Joint Research Center [7].

The weather station, placed close to the sampling station (Figure 2), consists of sensors to record the following parameters: Air temperature ($^{\circ}\text{C}$), relative humidity (%), pressure (mbar), irradiation (W/m^2), wind direction ($^{\circ}$), wind speed (m/s) and precipitation (mm). All these parameters are averaged over 10-minute intervals.

2.3. Backward Trajectories: HYSPLIT Model

The set of backward trajectories for the period 2009–2018 was calculated by using the HYSPLIT (Hybrid Single Particle Lagrangian Integrated Trajectory) model [25], with the meteorological input from the GDAS-NCEP model (Global Data Assimilation System—National Centers for Environmental Prediction), maintained by the NOAA/ARL (National Oceanic and Atmospheric Administration—Air Resources Laboratory's). The meteorological fields are provided with a temporal resolution of 6 h, a grid resolution of $1^{\circ} \times 1^{\circ}$ (in latitude and longitude), and 23 vertical levels (from 1000 to 20 hPa).

Two three-dimensional kinematic trajectories per day, computed at 00:00 and 12:00 UTC, with a run time of 96 h and with a final height of 100 m above ground level, were calculated during the studied period. A total of 6696 backward trajectories were used in this analysis. This large number of atmospheric trajectories provides a reliable representation of the synoptic/regional airflow patterns.

The present study uses the cluster analysis implemented in the HYSPLIT model to identify the airflow patterns, which is a multivariate statistical technique that groups trajectories with similar directions and lengths. The program uses the Ward's minimum variance clustering method to minimize the dissimilarity in the trajectories within each cluster, while maximizing the dissimilarity of different clusters [26]. Trajectories with similar horizontal and vertical paths are, hence, grouped together, forming clusters, taking as reference the spatial variance (SPVAR) of each cluster and the total spatial variance (TSV) between the different clusters [26]. The measure of dissimilarity is based on the horizontal path (latitude and longitude of each trajectory endpoint). In the present study, the optimal number of clusters, and hence, of airflow patterns, is associated with the step just before a variation of the TSV above 40% ("break point" in Stunder [26]). This technique has worked very well for discriminating distinct flow patterns and large-scale circulation features [27].

3. Results and Discussion

3.1. ^7Be Time Series Characterization

The first step to analyze the behavior of ^7Be in this area has been the representation of the measured values in chronological order (Figure 3a). The activity concentrations of ^7Be in the aerosols samples range from 7.3 to 0.35 mBq/m^3 , with a mean of $3.20 \pm 1.12 \text{ mBq}/\text{m}^3$, where the uncertainty is given as the sample standard deviation. This mean value coincides with the one presented in a previous study in Bilbao, $3.02 \pm 1.02 \text{ mBq}/\text{m}^3$ [22] and is coherent with those provided at similar latitudes, such as Granada ($4.86 \text{ mBq}/\text{m}^3$) [28], Lisbon ($4.0 \pm 2.0 \text{ mBq}/\text{m}^3$) [15].

The existence of outliers during this period has been studied by using the Grubbs test, which concludes that there are no outliers considering a significance standard level of $\alpha = 0.05$. Figure 3b displays the frequency distribution. A normal distribution has been fitted to, and its goodness has been tested using the Chi-square test. The observed chi-square test statistic is greater than the critical value, which allows us to conclude that ^7Be concentrations follow a normal distribution, similar to the one obtained in Todorovica [29] and Dueñas [30], but different, for instance, to the one presented in Lozano [17].

To analyze whether the ^7Be values, shown in Figure 3a, are a time series or noise [31], we have applied the simple autocorrelation test, which is designed to show the existence or not of a linear correlation between one observation and the next sequenced by time, and the intensity and type of this correlation.

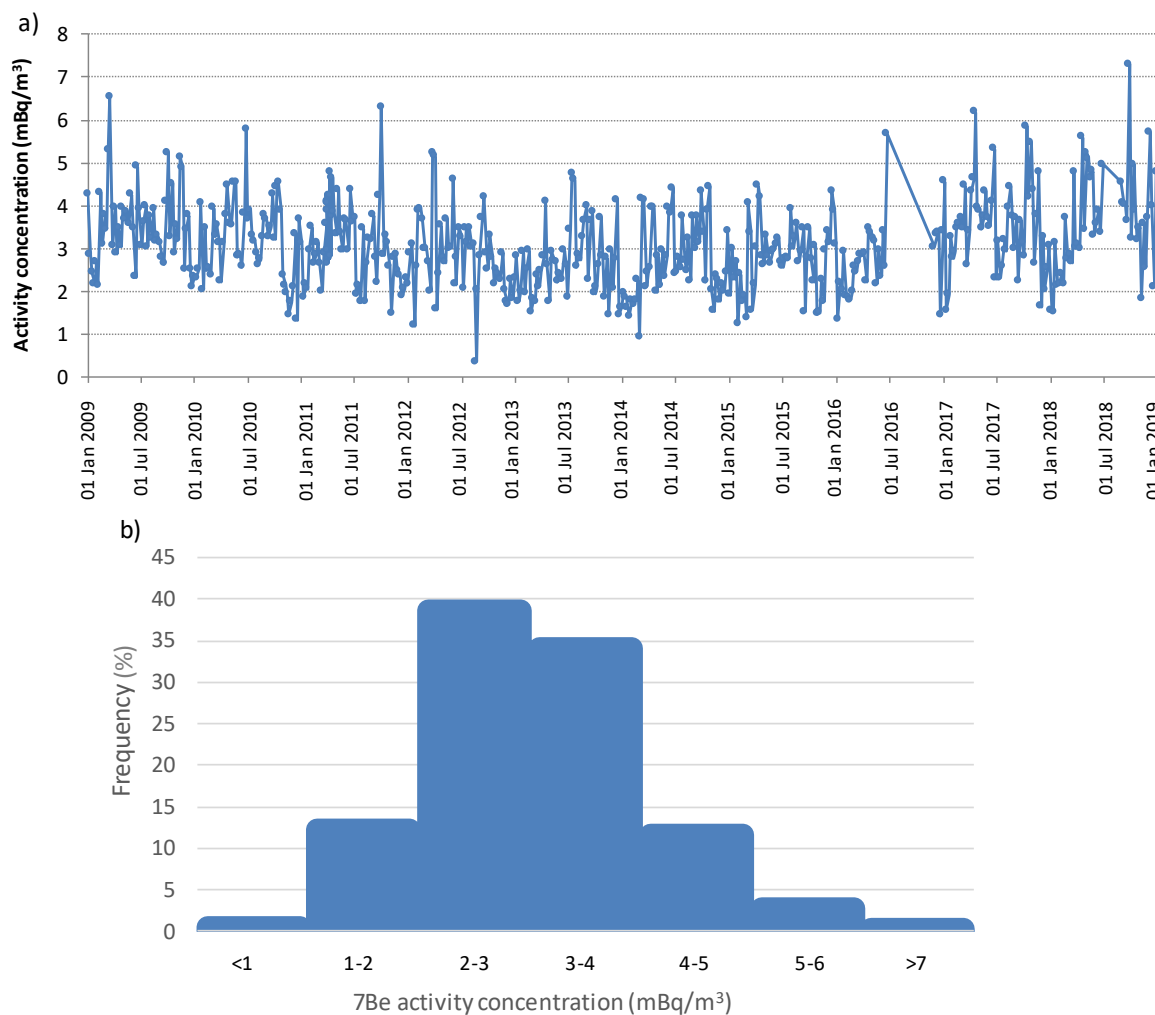


Figure 3. (a) Temporal variation and (b) histogram of the ⁷Be activity concentrations from January 2009 to December 2018 at Bilbao sampling station.

The test determines whether there is a statistical correlation between values of the series separated by increasing time-lapses. For stational series, a correlation will be observed when the time-lapse equals the stational period of the series. Hence, determining the time-lapse for which correlation is observed (correlation coefficient large than zero) it can be obtained the types of variation in the series (cyclical, stational).

It is possible to affirm that a simple autocorrelation of the variable exists when at least for a delay, the coefficient of autocorrelation is close or above the interval of confidence, as is shown in Figure 4. In the present study, it is seen that there are correlation delays of up to 12 weeks, which is associated with seasonal variability, and hence, it is possible to state that this set of data conforms to a time series [32,33].

Identifying dominant cyclical behaviors hidden in the ⁷Be time series of Bilbao is also addressed using the periodogram (Figure 5). Two peaks are clearly identified in the figure, one of them corresponding to a period around 10 years ($f = 1.93 \times 10^{-3}$) and the other one representing a period of 52 weeks (one year) ($f = 1.93 \times 10^{-2}$) [34,35]. Therefore, the results of this spectral analysis allow decomposing the ⁷Be time series into two main periodic components, 10 years cycle and annual.

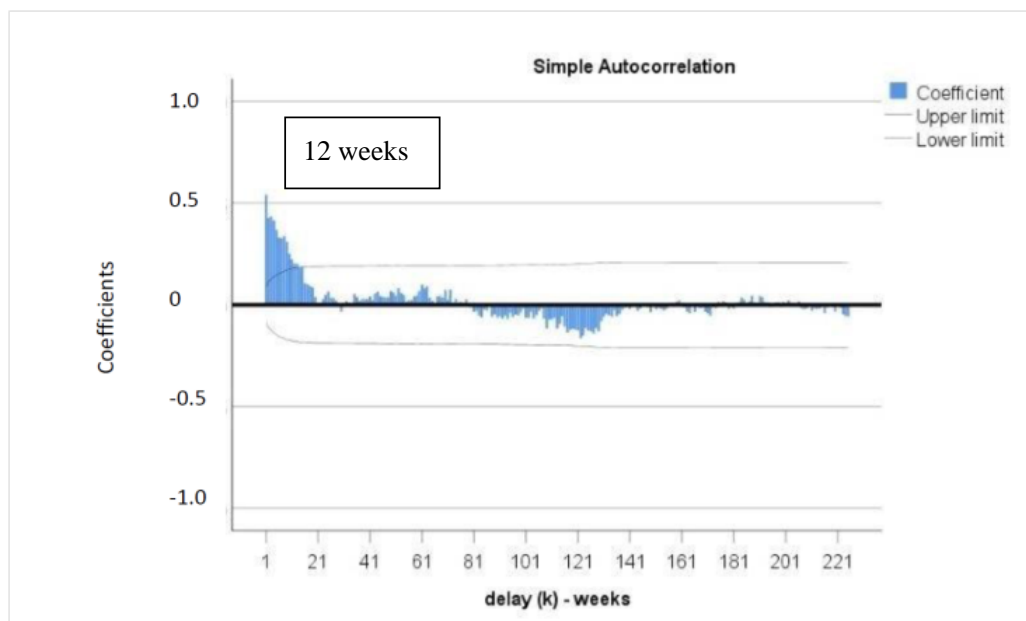


Figure 4. Representation of the simple autocorrelation test. The two lines indicate the confidence interval of 95%, and the bars are the coefficients of the analysis.

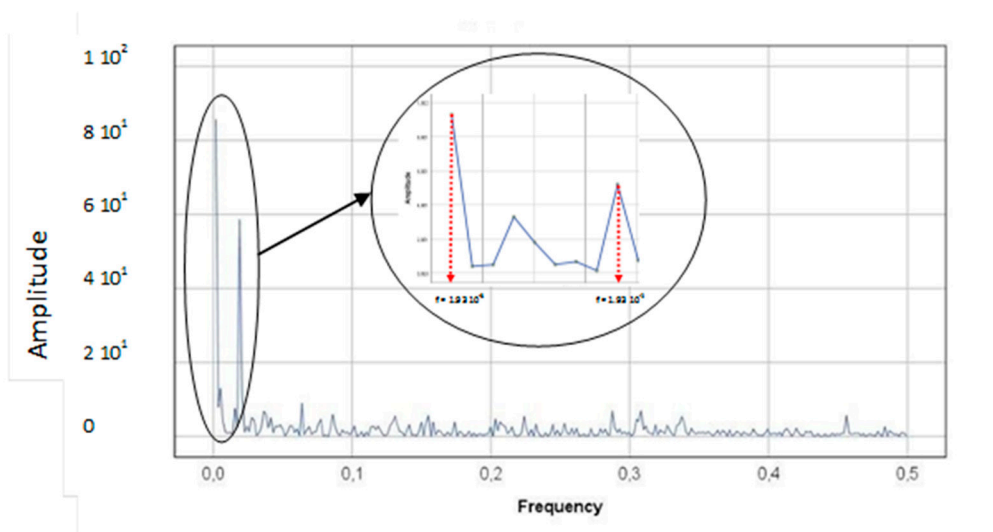


Figure 5. Periodogram for Bilbao time series of ⁷Be activity concentrations from 2009 to 2018.

These two components represent the long term pattern of the ⁷Be time series. Considering the annual average of ⁷Be during the ten years period (Figure 6), the time series shows a positive (increasing) long term pattern, 1.89×10^{-2} mBq/m³ year. This figure shows the progressive drop of annual ⁷Be concentrations from 2008 to 2013, similar values from 2014 to 2016, to finalize with a fast increase in 2017 and 2018. This inter-annual variability is closely driven by the cyclical component, which represents the periodic oscillations of ⁷Be concentrations following the solar cycle. Due to the production of ⁷Be through the interaction of cosmic rays with atmospheric molecules, its production rate varies with solar modulation of galactic cosmic rays invading the heliosphere [36], which is controlled by the solar magnetic field, and in turn, by solar activity [37]. The impact of the 11-year solar modulation on the ⁷Be concentrations in the air has been widely documented [38,39]. Figure 6 shows the annual number of sunspots within the previous solar cycle (24th solar cycle), which began in 2008 and ended between 2019 and 2020, with minimal activity until early 2010. The cycle featured a “double-peaked”

solar maximum, with the first peak reached in 2011 and the second in 2014. The Pearson’s correlation coefficient between the annual average of ^7Be and the number of sunspots is -0.93 , which confirms the strong inverse correlation between both variables.

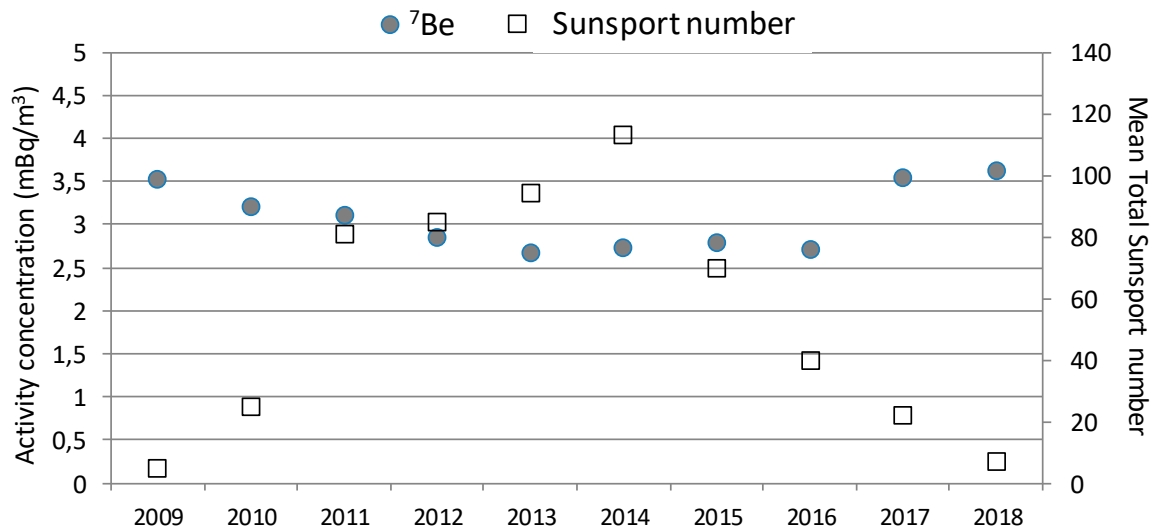


Figure 6. Yearly variations in the ^7Be activity concentration in Bilbao and sunspot number from 2009 to 2018 (Note: Sampling station failed during summer 2016).

The periodic oscillations within one year period are also analyzed. Seasonal and monthly averages during the whole period are shown in Figure 7, considering Winter (December, January, February), Spring (March, April, and May), Summer (June, July, and August) and Autumn (September, October, and November). This seasonal pattern, with higher concentrations during the warm season (spring-summer) and lower during the cold ones (autumn-winter) (Figure 7a), is well-known and is often observed at mid-latitudes sites [34,35,40]. This behavior can be associated with the seasonal variation of rainfall and with the vertical transport of ^7Be from the upper troposphere to the middle and lower troposphere during the spring-summer months [41]. In this sense, the correlation coefficient between the seasonal average of ^7Be and the total amount of precipitation in each season is -0.57 , which provides insight into how the precipitation plays a key role in the scavenging of this radionuclide.

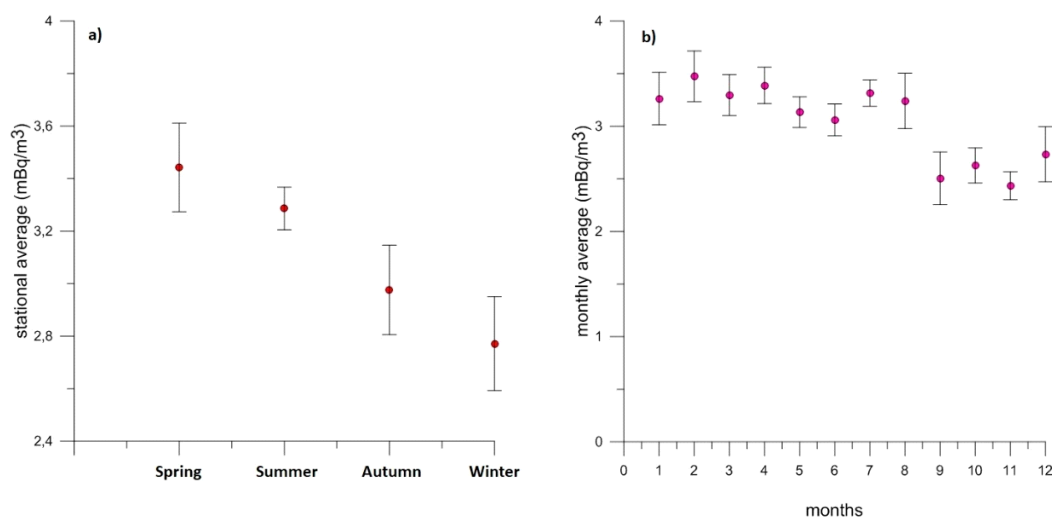


Figure 7. ^7Be activity concentrations, and 1σ error bars, on (a) seasonal and (b) monthly basis from 2009 to 2018.

The analysis of ^7Be activity data on a monthly basis (Figure 7b) helps to understand the differences between seasons. On average, the ^7Be concentration leaps in January and remains high until September, with a maximum in February and a secondary maximum during the months of July–August. There is also a need to point out the large break, on average, in concentrations between August (3.24 mBq/m³) and September (2.50 mBq/m³). In the case of monthly values, the correlation coefficient with the total amount of precipitation in each month is -0.46 .

3.2. ^7Be Activity Concentrations and Their Correlation with Local Meteorological Factors.

During the 10 years analyzed in the present study, weekly ^7Be activity concentrations exhibited large variability (Figure 3a). In previous studies [28], this strong variability is partially explained by variations in atmospheric parameters, such as temperature, relative humidity, and precipitation. In the present analysis, to better understand the impact of these meteorological parameters on ^7Be activity concentrations, they have been grouped into six ranges, according to the boxplot graph presented in Figure 8a. The six ranges are the following, according to ^7Be activity concentrations: Less than P10 (49 values), between P10 and P25 (74 values), between P25 and P50 (124 values), between P50 and P75 (124 values), between P75 and P90 (74 values) and greater than P90 (51 values). This figure shows that there is an asymmetrical distribution (positively skewed) of the ^7Be values, i.e., the P75 is farther from the median than P25, as well as the average is greater than the P50, which denotes the prevalence of low ^7Be values, although with the large impact of occasional high ones, in agreement with what was found in Hernandez-Ceballos [23] for the 2001–2010 period.

Averages of temperature, relative humidity, and atmospheric pressure, and the total amount of precipitation for each sampling period were calculated for each sampling period. Figure 8b–e show the scatter plots and the corresponding Pearson correlation coefficients (PCC) of ^7Be activity concentrations and each meteorological parameter. These results show two clear types of behavior, the negative correlation of relative humidity, and precipitation with ^7Be concentration, and the positive with temperature and pressure, which is in agreement with previous studies [42]. Negative PCC values imply the removal of particles during precipitation and high relative humidity conditions, which increase the scavenging effect and the gravimetric deposition of aerosols, and hence, decrease the ^7Be levels at ground level. On the contrary, the positive PCC values in temperature and pressure would mean enhancing convection processes during warm months in which high-pressure systems (e.g., Azores system) usually determine atmospheric conditions in the area. The highest correlation is obtained with precipitation ($r = -0.37$). Figure 9 shows that the highest ^7Be concentrations coincided with dry periods. This result, together with those obtained for the seasonal and monthly analysis, implies that precipitation is one of the factors controlling the concentration of ^7Be in Bilbao, in line with other different locations [15,43,44].

These low correlation values would also imply that other atmospheric processes should be included in the equation to better understand the surface concentration of ^7Be in Bilbao. As most of ^7Be come from the upper atmosphere [45], ^7Be concentrations are also influenced by changes in atmospheric production rates, due to the solar activity (Section 3.1 of the present paper), the stratosphere-troposphere exchange [23], and the advection processes [4]. A comprehensive analysis of advection patterns and surface winds is addressed in the next section.

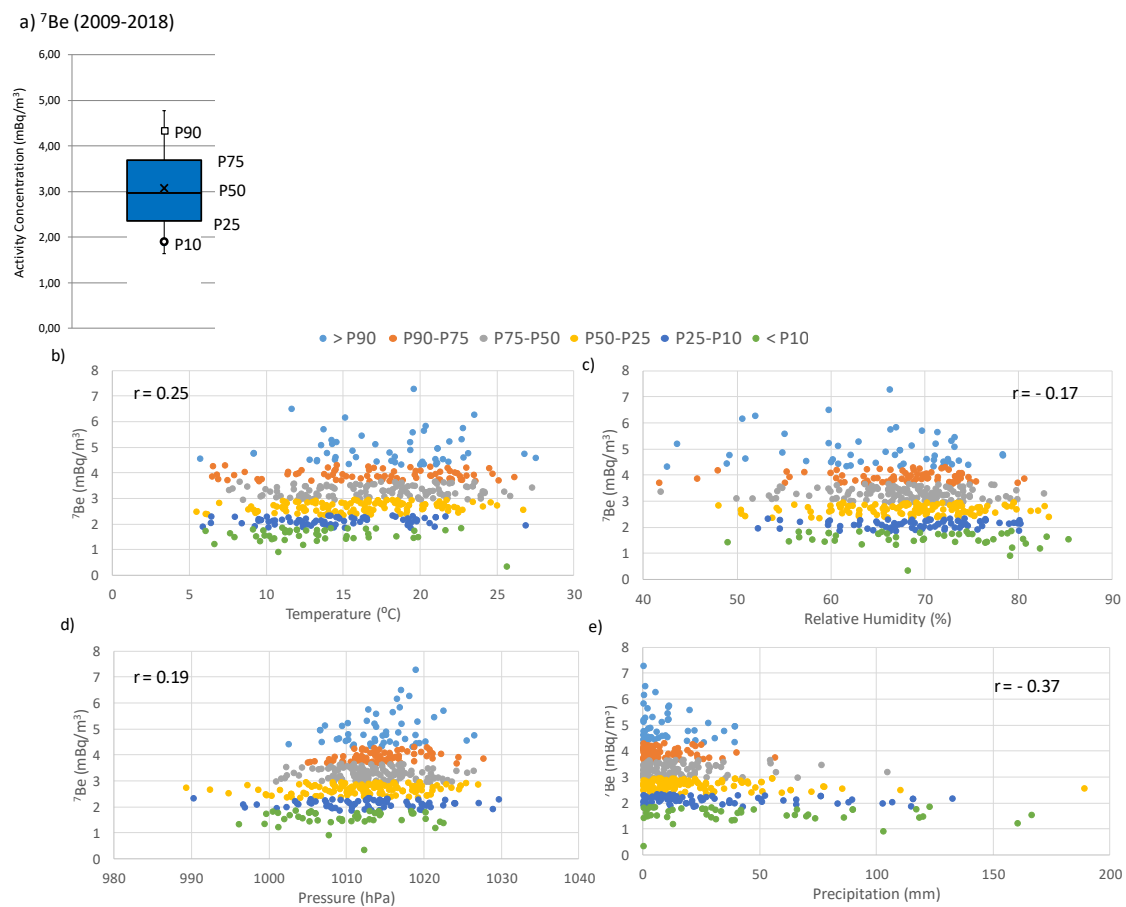


Figure 8. (a) Box-and-whisker plot of ^7Be activity concentrations from January 2009 to December 2018 at Bilbao sampling station, and the relationship between ^7Be concentration and meteorological parameters, (b) temperature, (c) relative humidity, (d) pressure, and (e) precipitation. In the center of the box denotes the 50% (P50), and the bottom and top of the box correspond to the 25% (P25) and 75% (P75) values, respectively. The square indicates the P90 and the circle the P10 values, while the extremes of the box represent the P95 and P5 values. The black cross is the average value.

3.3. Meteorological Scenarios and ^7Be Activity Concentrations: From Synoptic to Local

The set of meteorological synoptic/regional scenarios associated with ^7Be activity concentrations at Bilbao is presented in this section by clustering the backward trajectories calculated for all sampling periods according to ^7Be ranges. Figure 9 shows the average displacement of each airflow pattern for each ^7Be range. This figure shows the trajectories that are found to be clustered into a different number of airflow patterns at each ^7Be range, but at the same time, there are no large differences in airflow patterns or in their frequencies between ^7Be ranges. Taking as reference the origin and the average pathways followed by each airflow pattern, most of the cluster corresponding to westerly (W), northwesterly (NW), and northerly (N) flows, which, according to the length of the 96-hour trajectories in each cluster, can be grouped into, fast (WF, NWF, and NF) and slow (NWS, NS). The remaining trajectories are then grouped into a cluster representing slow continental southerly flows (SS).

WF assembles maritime air masses generated over the Atlantic Ocean coming from similar latitudes of Bilbao, NWF represents Atlantic air masses from high latitudes, while NWS collects those maritime air masses with a slower and shorter displacement. Northern cluster groups air masses originated over the North Sea (NS), as well as maritime arctic air masses (NF), and finally, SS represents continental air masses coming from the south with origin over the Iberian Peninsula. This variety of airflows is in agreement with the influence and the variability in displacement and

intensity of the Azores high-pressure center and the Icelandic low over synoptic circulations in the Iberian Peninsula [46].

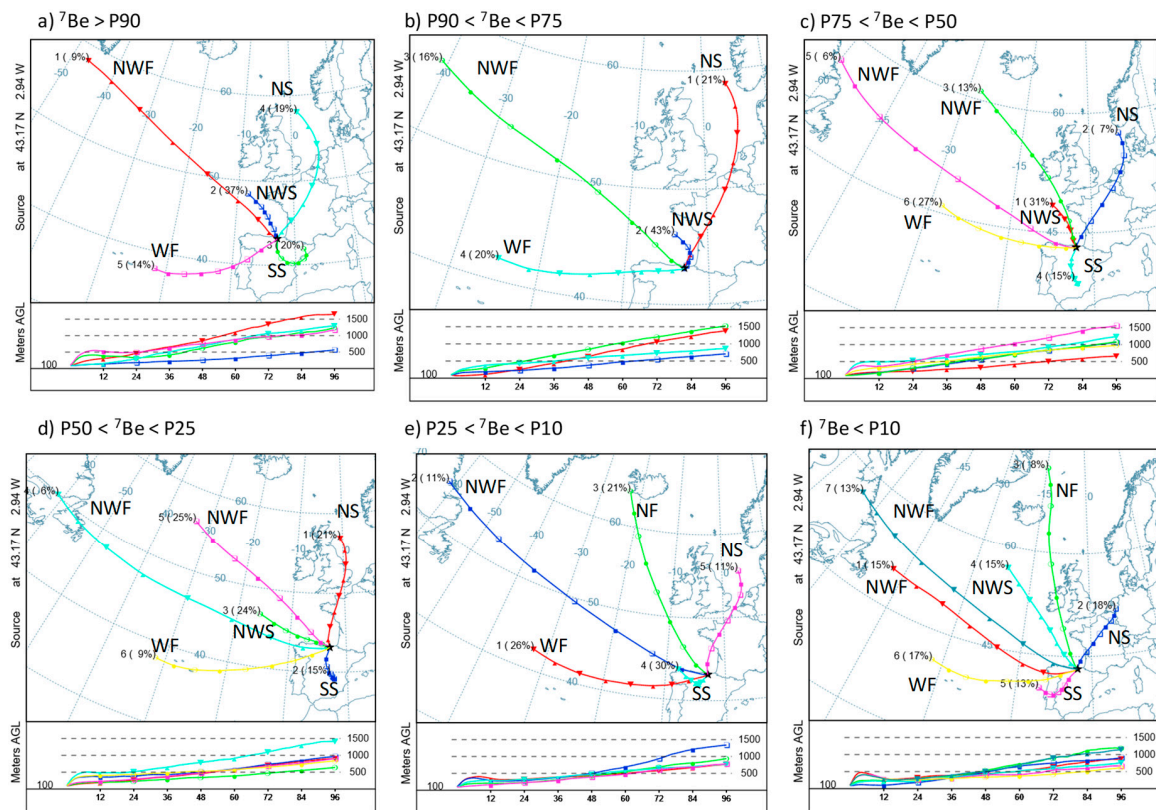


Figure 9. Back-trajectory cluster centers (centroids) were obtained at 100 m agl for the six ^7Be activity ranges at Bilbao. The left numbers in the centroids are an identification number of the centroid, and the right numbers (in brackets) are the percentage of complete trajectories occurring in that cluster.

In order to better characterize the relationships between airflow patterns and ^7Be concentrations, persistent sampling periods were taken as reference, i.e., those sampling periods attributed to only one advection pattern (when at least 60% of the trajectories ending at Bilbao during one single sampling period belong to the same airflow pattern). This quality criterion is applied in other studies, such as Brattich [47], in which relationships between advection pathways and atmospheric composition at the high-mountain station of Mt. Cimone (Italy) are analyzed. This assumption is taken to avoid the possibility of considering the same sampling period in the results of two different airflow patterns, which would increase the uncertainty in the results. Figure 10 shows the total number of persistent periods within each airflow pattern, and their corresponding monthly frequency. In total, we are working with 239 sampling periods (48% of total sampling periods within the period 2009–2018). From now on, only persistent periods are considered.

Aiming now to shed light on the relationship between airflow patterns and ^7Be activity concentrations in Bilbao, Figure 11 shows the correlation coefficients between monthly specific activities of ^7Be and the frequency of airflow patterns arriving at Bilbao. In this figure, a positive (negative) correlation coefficient indicates an increase (decrease) in aerosol concentration, due to the more frequent arrival of an airflow pattern [48]. Only correlation coefficients with a p -value < 0.05 are highlighted in the figure, and it can be appreciated that there are three airflow patterns presenting a correlation value statistically significant, two negatives, NF with -0.55 and NWF with -0.80 , and one positive, NWS with 0.70 . Figure 12 also shows the monthly specific activity for ^7Be and the monthly frequency for these airflow patterns. While NF presents the highest frequencies in the cold months, in the case of NWF, its highest monthly occurrence coincides with falls in ^7Be concentrations. On the

contrary, the monthly evolutions of the NWS pattern and ^7Be properly fit well, presenting higher values and frequencies in the spring and summer months. In this sense, it is interesting to remark the second peak of ^7Be monthly concentrations observed in September–October, which is in line with the results obtained in Ajtic [49] in which is reported a high percentage (23%) of ^7Be activity concentrations above the 95th percentile in autumn at Bilbao. The influence of this airflow pattern could be, hence, related to high ^7Be concentrations, which are normally assigned to the thinning of the tropopause resulting in air exchange between the stratosphere and troposphere. Several authors have identified the northern Atlantic as one of the most important areas associated with high ^7Be activity concentration measured in Europe [50].

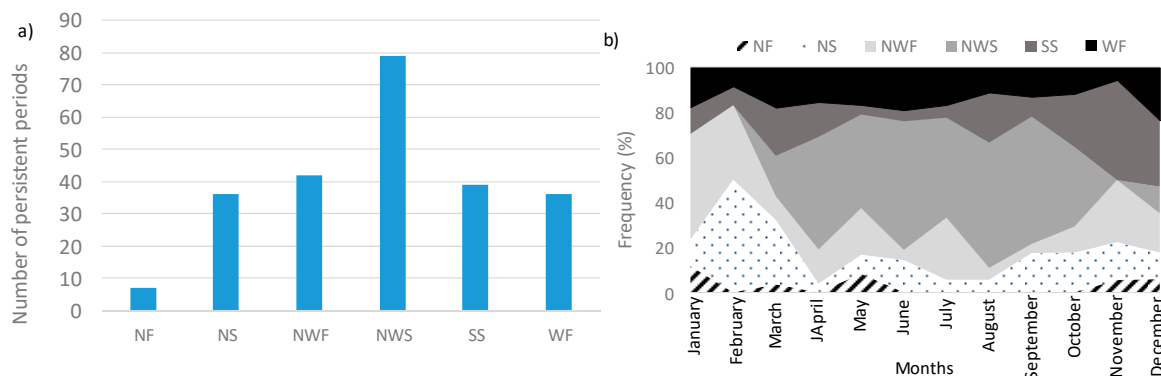


Figure 10. (a) The number of persistent periods within each airflow pattern, and (b) monthly frequency during the 2009–2018 period.

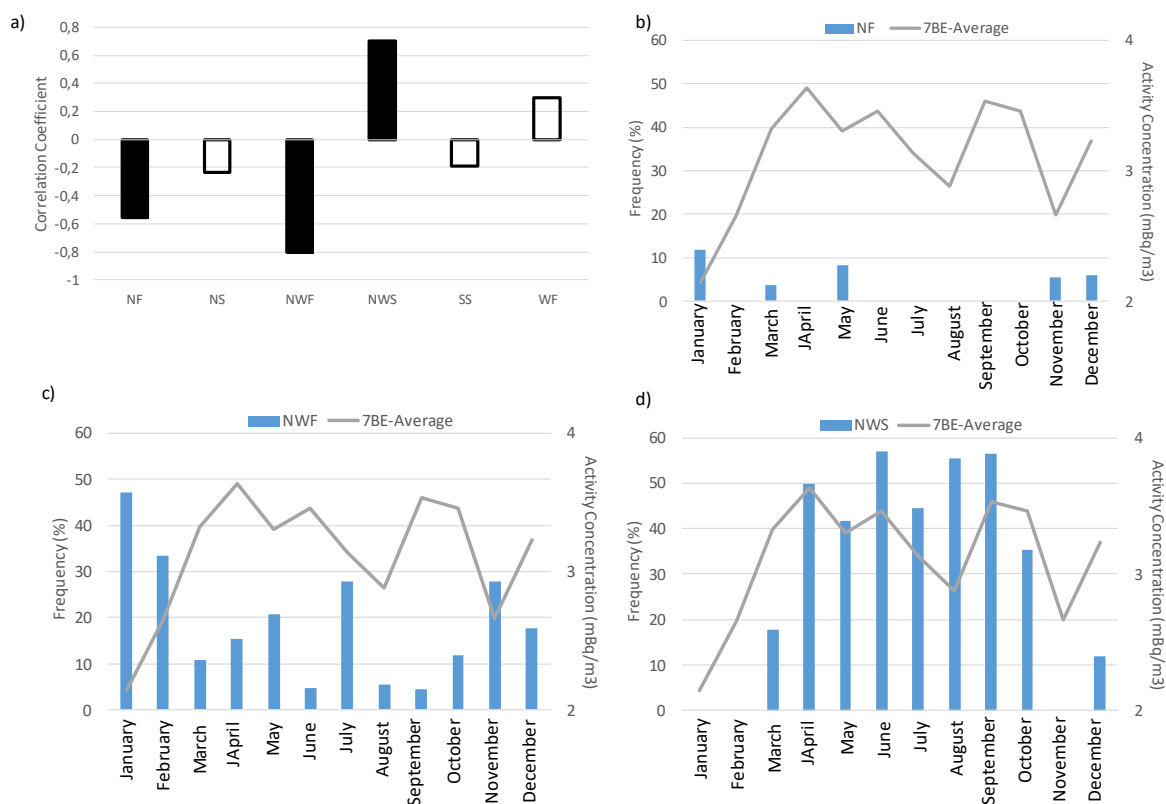


Figure 11. (a) Correlation coefficients of the monthly ^7Be activities and airflow patterns (Only correlation coefficients with a p -value < 0.05 are highlighted in the figure), and monthly specific activities for ^7Be and their relationship to the monthly frequency of (b) NF, (c) NWF, and (d) NWS flows. Only persistent sampling periods are used.

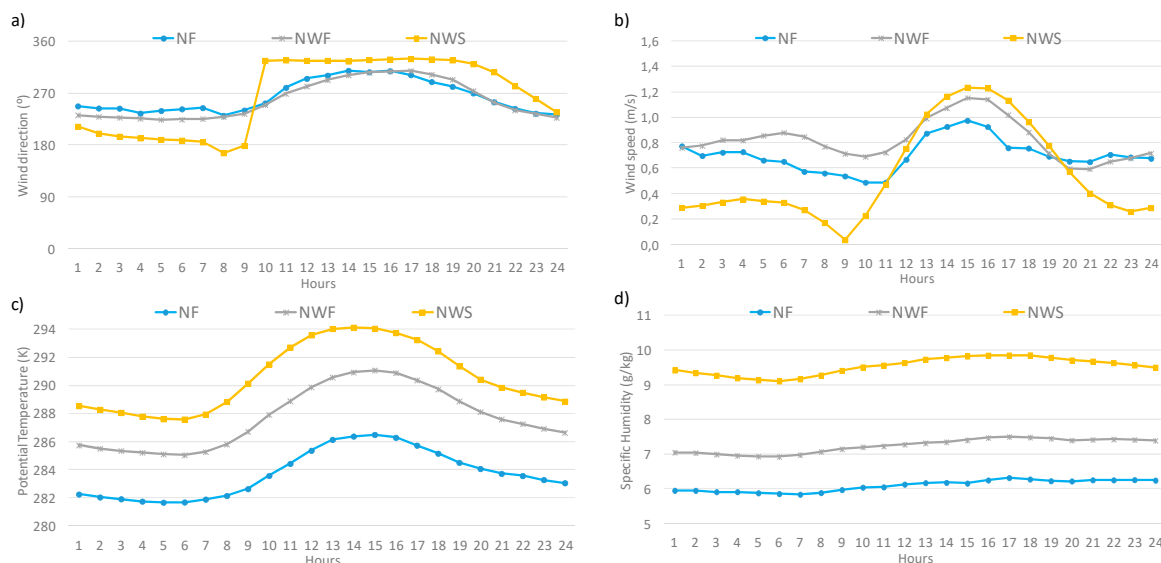


Figure 12. Daily cycles of (a) wind direction and (b) speed, (c) potential temperature, and (d) specific humidity associated with different airflow patterns at Bilbao. Only persistent sampling periods are used.

The present analysis with trajectories has, however, limitations to represent mesoscale and local flows, which are key to understand ground-level concentrations of ⁷Be. In this sense, the geographical characteristics of the sampling site, and the resulting mesoscale and local processes developed, modulate the impact of synoptic processes on ⁷Be, and hence, there is a need to complement the previous analysis with meteorological information measured at the site, to establish a link between synoptic/regional and mesoscale/local processes. Figure 12 presents the daily cycles of wind direction and speed, specific humidity, and potential temperature for each one of the three airflow patterns (NF, NWF, NWS) previously identified with a significant impact on ⁷Be activity concentrations. Potential temperature and specific humidity are calculated, and are treated as a transport tracer that follows a specific air mass. The calculation of these daily cycles is based only on persistent periods.

As shown, there are clear differences in surface measurements and daily cycles among them. The daily cycles of potential temperature and specific humidity indicate, for instance, differences at about 8 K and 4 g/Kg between NWS (warm and wet) and NF (cold and dry), which are associated with the different origin and type of displacement to Bilbao. A very important difference between them, which may justify the temporal variability of ⁷Be activity concentrations, is observed in the surface wind regime. While the arrival of NF and NWF airflows presents a prevalence of surface winds from the northwest, the NWS pattern shows an hourly evolution with a nocturnal flow from the south until 10:00, when the winds begin to blow from the northwest, remaining until 21:00, when they start changing to southerly again. Differences in wind speed are also clearly shown, with data ranged from 1.10 to 0.5 m/s in NF and NWF, and from 1.20 to 0.1 m/s.

The characteristics of surface winds under the arrival of NF and NWF are favorable to the dispersion mechanism at ground level. However, the daily evolution of winds at a surface level associated with the arrival of NWS flows agrees with the development of sea/land breezes in this area [51], which are more common during spring and summer. Many studies have demonstrated the impact of sea/land breezes on quality air [52,53], because it traps the particles near the surface in a recirculation mechanism, limiting a sufficient mixing with the air above, and hence, the dispersion processes in the lower atmosphere. In this case, and in the light of these results, we could indicate that the interaction of this local phenomenon with the prevailing NWS airflows produces a specific atmospheric condition that would increase ⁷Be activity concentration in this area.

4. Conclusions

Our study looked into the description of ^7Be activity concentrations measured in the Bilbao sampling station from 2009 to 2018 and its link with meteorological parameters.

After analyzing all results, it can be concluded that ^7Be weekly concentration in Bilbao can be considered a time series. This is made up of a practically horizontal trend line with a slope of 1.89×10^{-2} mBq/m³ year, a cyclical component that follows the solar cycle with a correlation coefficient of -0.93 , and a marked seasonal component that follows rainfall distribution showing low concentrations when rainfall, and hence, scavenging is at its maximum, i.e., November and December.

In order to explain the irregular component of the ^7Be time series, the link between ^7Be and meteorological parameters at a local scale was analyzed. In this sense, a general impression is the weak correlation of ^7Be with meteorological factors, which is mainly associated with the use of weekly ^7Be values as a reference to perform the analysis. Under this perspective, the present set of results evidenced that precipitation is the main factor controlling the concentration of ^7Be in Bilbao. The study of the airflow patterns and surface winds pointed out that high ^7Be concentrations would be associated with the arrival of air masses from the northwest (northern Atlantic), and the development of sea/land breezes in this area, which limit the dispersion processes and hence, the increase of ^7Be activity concentrations in the area. These results can be taken as the first step to go into detail regarding the influence of local-mesoscale-synoptic meteorological conditions on radioactivity levels in the area, e.g., the impact of sea-land breezes, as well as this database could be used to investigate the modification of circulation patterns because of climate change.

Author Contributions: Conceptualization, N.A.; Formal analysis, N.A. and M.Á.H.-C.; Methodology, N.A.; Software, N.A.; Writing—original draft, N.A. and M.Á.H.-C.; Writing—review & editing, N.A., M.Á.H.-C., M.H., R.I. and F.L. All authors have read and agreed to the published version of the manuscript.

Funding: This research received no external funding.

Acknowledgments: The authors gratefully acknowledge the NOAA Air Resources Laboratory (ARL) for the provision of the HYSPLIT transport and dispersion model and/or READY website (<https://www.ready.noaa.gov>) used in this publication.

Conflicts of Interest: The authors declare no conflict of interest.

References

1. Gaffney, J.S.; Marley, N.; Cunningham, M.M. Natural radionuclides in fine aerosols in the Pittsburgh area. *Atmos. Environ.* **2004**, *38*, 3191–3200. [[CrossRef](#)]
2. Kulan, A.; Aldahan, A.; Possnert, G.; Vintersved, I. Distribution of ^7Be in surface air of Europe. *Atmos. Environ.* **2006**, *40*, 3855–3868. [[CrossRef](#)]
3. Piñero-García, F.; Ferro-García, M.A.; Chham, E.; Cobos-Díaz, M.; Gonzalez-Rodelas, P. A cluster analysis of back trajectories to study the behavior of radioactive aerosols in the south-west of Spain. *J. Environ. Radioact.* **2015**, *147*, 142–152. [[CrossRef](#)] [[PubMed](#)]
4. Brattich, E.; Liu, H.; Tositti, L.; Considine, D.B.; Crawford, J.H. Processes controlling the seasonal variations in ^{210}Pb and ^7Be at the Mt. Cimone WMO-GAW global station, Italy: A model analysis. *Atmos. Chem. Phys.* **2017**, *17*, 1061–1080. [[CrossRef](#)]
5. CTBTO Preparatory Commission. Available online: <https://www.ctbto.org/> (accessed on 5 November 2020).
6. REM Web Site. Available online: <https://rem.jrc.ec.europa.eu/RemWeb/> (accessed on 1 November 2020).
7. Sangiorgi, M.; Hernández-Ceballos, M.A.; Iurlaro, G.; Cinelli, G.; De Cort, M. 30 years of European Commission Radioactivity Environmental Monitoring data bank (REMdb)—An open door to boost environmental radioactivity research. *Earth Syst. Sci. Data* **2019**, *11*, 589–601. [[CrossRef](#)]
8. Leppanen, A.-P.; Pacini, A.A.; Usoskin, I.G.; Aldahan, A.; Echer, E.; Evangelista, H.; Klemola, S.; Kovaltsov, G.A.; Mursula, K.; Possnert, G. Cosmogenic ^7Be in air: A complex mixture of production and transport. *J. Atmos. Solar Terr. Phys.* **2010**, *72*, 1036–1043. [[CrossRef](#)]

9. Usoskin, I.; Kovaltsov, G. Production of cosmogenic ^7Be iso-tope in the atmosphere: Full 3D modelling. *J. Geophys. Res.* **2008**, *113*, D12107. [[CrossRef](#)]
10. Kikuchi, S.; Sakurai, H.; Gunji, S.; Tokanai, F. Temporal variation of ^7Be concentrations in atmosphere for 8y from 2000 at Yamagata, Japan: Solar influence on the ^7Be time series. *J. Environ. Radioact.* **2009**, *100*, 515–521. [[CrossRef](#)]
11. Ioannidou, A.; Papastefanou, C. Precipitation scavenging of ^7Be and ^{137}Cs radionuclides in air. *J. Environ. Radioact.* **2006**, *85*, 121–136. [[CrossRef](#)]
12. Liu, H.; Considine, D.B.; Horowitz, L.W.; Crawford, J.H.; Rodriguez, J.M.; Strahan, S.E.; Damon, M.R.; Steenrod, S.D.; Xu, X.; Kouatchou, J.; et al. Using beryllium-7 to assess cross-tropopause transport in global models. *Atmos. Chem. Phys.* **2016**, *16*, 4641–4659. [[CrossRef](#)]
13. Hernández-Ceballos, M.A.; Brattich, E.; Cinelli, G.; Ajtic, J.; Djurdjevic, V. Seasonality of ^7Be concentrations in Europe and influence of tropopause height. *Tellus B Chem. Phys. Meteorol.* **2016**, *68*, 29534. [[CrossRef](#)]
14. Grossi, C.; Ballester, J.; Serrano, I.; Galmarini, S.; Camacho, A.; Curcoll, E.; Morguá, J.A.; Rodo, X.; Duch, M.A. Influence of long-range atmospheric transport pathways and climate teleconnection patterns on the variability of surface ^{210}Pb and ^7Be concentrations in southwestern Europe. *J. Environ. Radioact.* **2016**, *165*, 103–114. [[CrossRef](#)] [[PubMed](#)]
15. Carvalho, A.C.; Reis, M.; Silva, L.; Madruga, M.J. A decade of ^7Be and ^{210}Pb activity in surface aerosols measured over the Western Iberian Peninsula. *Atmos. Environ.* **2013**, *67*, 193–202. [[CrossRef](#)]
16. Bas Cerdá, M.D.C.; Ortiz Moragón, J.; Ballesteros Pascual, L.; Martorell Alsina, S.S. Analysis of the influence of solar activity and atmospheric factors on Be-7 air concentration by seasonal-trend decomposition. *Atmos. Environ.* **2016**, *145*, 147–157. [[CrossRef](#)]
17. Lozano, R.L.; Hernández-Ceballos, M.A.; San Miguel, E.G.; Adame, J.A.; Bolívar, J.P. Meteorological factors influencing on surface air ^7Be and ^{210}Pb concentrations from southwestern Iberian Peninsula. *Atmos. Environ.* **2012**, *63*, 168–178. [[CrossRef](#)]
18. San Miguel, E.G.; Hernández-Ceballos, M.A.; García-Mozo, H.; Bolívar, J.P. Evidences of different meteorological patterns governing ^7Be and ^{210}Pb surface levels in the southern Iberian Peninsula. *J. Environ. Radioact.* **2019**, *198*, 1–10. [[CrossRef](#)]
19. Gordo, E.; Liger, E.; Duenas, C.; Fernandez, M.C.; Canete, S.; Perez, M. Study of ^7Be and ^{210}Pb as radiotracers of african intrusions in Malaga (Spain). *J. Environ. Radioact.* **2015**, *148*, 141–153. [[CrossRef](#)]
20. Dueñas, C.; Gordo, E.; Liger, E.; Cabello, M.; Cañete, S.; Pérez, M.; De la Torre-Luque, P. ^7Be , ^{210}Pb and ^{40}K depositions over 11 years in Málaga. *J. Environ. Radioact.* **2017**, *178–179*, 325–334. [[CrossRef](#)]
21. Piñero-García, F.; Ferro-García, M.A.; Azahra, M. ^7Be behaviour in the atmosphere of the city of Granada January 2005 to December 2009. *Atmos. Environ.* **2012**, *47*, 84–91. [[CrossRef](#)]
22. Alegria, N.; Herranz, M.; Idoeta, R.; Legarda, F. Study of ^7Be activity concentration in the air of northern Spain. *J. Radioanal. Nucl. Chem.* **2010**, *286*, 347–351. [[CrossRef](#)]
23. Hernandez-Ceballos, M.A.; Brattich, E.; Lozano, L.; Cinelli, G. ^7Be behaviour and meteorological conditions associated with ^7Be peak events in Spain. *J. Environ. Radioact.* **2017**, *166*, 17–26. [[CrossRef](#)] [[PubMed](#)]
24. Datos Climáticos Mundiales. Available online: <https://es.climate-data.org/> (accessed on 5 November 2020).
25. Stein, A.F.; Draxler, R.R.; Rolph, G.D.; Stunder, B.J.B.; Cohen, M.D.; Ngan, F. NOAA's HYSPLIT atmospheric transport and dispersion modeling system. *Bull. Am. Meteorol. Soc.* **2015**, *96*, 2059–2077. [[CrossRef](#)]
26. Stunder, B. An assessment of the quality of forecast trajectories. *J. Appl. Meteorol.* **1996**, *35*, 1319–1331. [[CrossRef](#)]
27. Hernández-Ceballos, M.A.; Adame, J.A.; Bolívar, J.P.; De la Morena, B.A. Vertical behaviour and meteorological properties of air masses in the southwest of the Iberian Peninsula (1997–2007). *Meteorol. Atmos. Phys.* **2013**, *119*, 163–175. [[CrossRef](#)]
28. Chham, E.; Milena-Pérez, A.; Piñero-García, F.; Hernández-Ceballos, M.A.; Orzae, A.G.; Brattich, E.; El Bardouni, T.; Ferro-García, A. Sources of the seasonal-trend behaviour and periodicity modulation of ^7Be air concentration in the atmospheric surface layer observed in southeastern Spain. *Atmos. Environ.* **2019**, *213*, 148–158. [[CrossRef](#)]
29. Todorovica, D.; Popovic, D.; Djuric, G.; Radenkovic, M. ^7Be to ^{210}Pb concentration ratio in ground level air in Belgrade area. *J. Environ. Radioact.* **2005**, *79*, 297–307. [[CrossRef](#)]
30. Dueñas, C.; Fernández, M.C.; Cañete, S.; Pérez, M. ^7Be to ^{210}Pb concentration ratio in ground level air in Málaga (36.7° N, 4.5° W). *Atmos. Res.* **2009**, *92*, 49–57. [[CrossRef](#)]

31. Kendall, M. *Time Series*; Charles Griffin: London, UK, 1976; ISBN 0-85264-241-5.
32. Hewitt, C.N. *Methods of Environmental Data Analysis*; Elsevier Applied Science: London, UK, 1992; ISBN 978-94-010-9514-3.
33. Chatfield, C. *The Analysis of Time Series: Theory and Practice*; Chapman and Hall: London, UK, 1975; ISBN 0-412-31820-2.
34. Ioannidou, A.; Papastefanou, C. Beryllium-7 concentrations in the lower atmosphere at the region of Thessaloniki (40° N). *HNPS Proc.* **1994**, *5*, 185–195. [[CrossRef](#)]
35. Ishikawa, Y.; Murakami, H.; Sekine, T.; Yoshirara, K. Precipitation Scavenging Studies of Radionuclides in Air Using Cosmogenic ⁷Be. *J. Environ. Radioact.* **1995**, *26*, 19–26. [[CrossRef](#)]
36. Masarik, J.; Beer, J. Simulation of particle fluxes and cosmogenic nuclide production in the Earth's atmosphere. *J. Geophys. Res. Atmos.* **1999**. [[CrossRef](#)]
37. Cinelli, G.; De Cort, M.; Tollefsen, T. (Eds.) *European Atlas of Natural Radiation*; Publication Office of the European Union: Luxembourg, 2019; ISBN 978-92-76-08259-0. [[CrossRef](#)]
38. Leppanen, A.P.; Paatero, J. ⁷Be in Finland during the 1999–2001 Solar maximum and 2007–2009 Solar minimum. *J. Atmos. Sol. Terr. Phys.* **2013**, *97*, 1–10. [[CrossRef](#)]
39. Hernández-Ceballos, M.A.; Cinelli, G.; Marín Ferrer, M.; Tollefsen, T.; De Felice, L.; Nweke, E.; Tognoli, P.V.; Vanzo, S.; De Cort, M. A climatology of ⁷Be in surface air in European Union. *J. Environ. Radioact.* **2015**, *141*, 62–70. [[CrossRef](#)] [[PubMed](#)]
40. Valles, I.; Camacho, A.; Ortega, X.; Serrano, I.; Blazquez, S.; Pérez, S. Natural and anthropogenic radionuclides in airborne particulate samples collected in Barcelona Spain. *J. Environ. Radioact.* **2009**, *100*, 102–107. [[CrossRef](#)] [[PubMed](#)]
41. Baskaran, M. A search for the seasonal variability on the depositival fluxes of ⁷Be and ²¹⁰Pb. *J. Geophys. Res. Atmos.* **1995**, *100*, 2833–2840. [[CrossRef](#)]
42. Pham, M.; Betti, M.; Nies, H.; Povinec, P. Temporal changes of ⁷Be, ¹³⁷Cs and ²¹⁰Pb activity concentrations in surface air at Monaco and their correlation with meteorological parameters. *J. Environ. Radioact.* **2011**, *102*, 1045–1054. [[CrossRef](#)] [[PubMed](#)]
43. Azahra, M.; Camacho-García, A.; González-Gómez, C.; López-Peñalver, J.J.; El Bardouni, T. Seasonal ⁷Be concentrations in near-surface air of Granada (Spain) in the period 1993–2001. *Appl. Radiat. Isot.* **2003**, *59*, 159–164. [[CrossRef](#)]
44. Tositti, L.; Brattich, E.; Cinelli, G.; Baldaccia, D. 12 years of ⁷Be and ²¹⁰Pb in Mt. Cimone, and their correlation with meteorological parameters. *Atmos. Environ.* **2014**, *87*, 108–122. [[CrossRef](#)]
45. Yoshimori, M.; Hirayama, H.; Mori, S.; Sasaki, K.; Sakurai, H. Be-7 nuclei produced by galactic cosmic rays and solar energetic particles in the earth's atmosphere. *Adv. Space Res.* **2013**, *32*, 2691–2696. [[CrossRef](#)]
46. Font Tullot, I. *Climatología de España y Portugal (Nueva Versión)*; Universidad de Salamanca: Salamanca, Spain, 2000; ISBN1 8478009442. ISBN2 9788478009442.
47. Brattich, E.; Orza, J.A.G.; Cristofanelli, P.; Bonasoni, P.; Marinoni, A.; Tositti, L. Advection pathways at the Mt. Cimone WMO-GAW station: Seasonality, trends, and influence on atmospheric composition. *Atmos. Environ.* **2020**, *234*, 117513. [[CrossRef](#)]
48. Dueñas, C.; Orza, J.A.G.; Cabello, M.; Fernández, C.; Cañete, S.; Pérez, M.; Gordo, E. Air mass origin and its influence on radionuclide activities (⁷Be and ²¹⁰Pb) in aerosol particles at a coastal site in the western Mediterranean. *Atmos. Res.* **2011**, *101*, 205–214. [[CrossRef](#)]
49. Ajić, J.V.; Sarvan, D.; Djurdjevic, V.S.; Hernández-Ceballos, M.A.; Brattich, E. Beryllium-7 surface concentration extremes in Europe. *Facta Univ. Ser. Phys. Chem. Technol.* **2017**, *15*, 45–55. [[CrossRef](#)]
50. Zanis, P.; Shuepbach, E.; Gäggeler, H.W.; Huebener, S.; Tobler, L. Factors controlling beryllium-7 at Jungfraujoch in Switzerland. *Tellus B Chem. Phys. Meteorol.* **1999**, *51*, 789–805. [[CrossRef](#)]
51. Acero, J.A.; Arrizabalaga, J.; Kupski, S.; Katzschner, L. Urban heat island in a coastal urban area in northern Spain. *Theor. Appl. Climatol.* **2013**, *113*, 137–154. [[CrossRef](#)]
52. Ribeiro, F.N.D.; de Oliveira, A.P.; Soares, J.; de Miranda, R.M.; Barlage, M.; Chenc, F. Effect of sea breeze propagation on the urban boundary layer of the metropolitan region of Sao Paulo, Brazil. *Atmos. Res.* **2018**, *214*, 174–188. [[CrossRef](#)]

53. Mazzuca, G.M.; Pickering, K.E.; New, D.A.; Dreessen, J.; Dickerson, R.R. Impact of bay breeze and thunderstorm circulations on surface ozone at a site along the Chesapeake Bay 2011–2016. *Atmos. Environ.* **2019**, *198*, 351–365. [[CrossRef](#)]

Publisher’s Note: MDPI stays neutral with regard to jurisdictional claims in published maps and institutional affiliations.



© 2020 by the authors. Licensee MDPI, Basel, Switzerland. This article is an open access article distributed under the terms and conditions of the Creative Commons Attribution (CC BY) license (<http://creativecommons.org/licenses/by/4.0/>).